

Experimental comparison of discharge coefficient of A-type piano key and labyrinth side weirs with different heights

Saeid Jeddi¹ , Jalal Sadeghian^{*2} 

¹Department of Civil Engineering, Faculty of Engineering, University of Zanjan, Zanjan, Iran.

²Department of Civil Engineering, Faculty of Engineering, Bu-Ali Sina University, Hamedan, Iran.

GRAPHICAL ABSTRACT

The experimental models used in the present study included the triangular, trapezoidal and rectangular Labyrinth weirs and the piano key weir each considering 3 cycles and 4 heights of 5, 10, 15 and 20 cm and the piano key weirs were of type A.



10 m channel and side channel view



Side weirs models

ARTICLE INFO

Article type:

Research Article

Article history:

Received xx Month xxx

Received in revised form xx Month xxx

Accepted xx Month xxx

Available online x Month xx

Keywords:

Discharge coefficient

Labyrinth weir

Piano key weir

Side weir



© The Author(s)

Publisher: Razi University

ABSTRACT

Hydraulic structures have a long history, with weirs being among the earliest developed; a notable example of these is the side weir. Side weirs are of different shapes, including a nonlinear weir installed on the dam crest. Weirs with nonlinear designs come in various forms, like labyrinth and piano key weirs; these are used when weir length is restricted, to maximize crest length, which subsequently increases discharge capacity. This study examines and contrasts how piano key and labyrinth weirs function as side weirs, since there has been little research on piano key side weirs. Within this study, the experimental models incorporated trapezoidal, rectangular, and triangular Labyrinth weirs, alongside piano key weirs, each characterized by four distinct heights 5, 10, 15, and 20 cm and three cycles, where the piano key weirs were classified as A-type. At a certain H/P ratio, weirs with a smaller height had the maximum discharge coefficient and vice versa for weirs with a larger height. When a straight piano key weir and a rectangular labyrinth weir are both placed at a right angle to the stream, the piano key weir performs better. Conversely, the present study, which evaluated the aforementioned weirs as side weirs, yielded contrasting results; the rectangular labyrinth weir exhibited superior efficiency to the piano key weir. The study's findings revealed triangular labyrinth side weirs exhibited a superior discharge coefficient (maximum 0.689), while rectangular labyrinth weirs outperformed piano key weirs by up to 24.85 % in side-channel arrangements.

1. Introduction

Weirs represent some of the most fundamental and longstanding hydraulic structures, used for a variety of applications, including flow diversion, riverbank erosion mitigation, and water level regulation in reservoirs. The versatile functionality of side weirs has led to their widespread utilization in dams and canals. Given the critical role of side weirs, implementing designs with superior efficiency and discharge capacity is essential, causing a thorough investigation of flow behavior in these structures.

Labyrinth and piano key weirs represent significant examples of nonlinear side weir design. These designs are typically installed along the sidewalls of open channels or next to primary flow paths, addressing spatial constraints through their compact yet efficient geometry. By extending the effective crest length, these weirs substantially improve

the discharge coefficient, rendering them suitable for applications requiring effective flow management within limited spaces. The operational efficacy of piano key and labyrinth weirs is contingent upon geometric attributes, including weir height, angle, cycle quantity, thickness, and crest configuration, which critically affect efficiency (Anderson and Tullis, 2012). Furthermore, hydraulic parameters such as input discharge, flow velocity and type, water depth, and surface profile also play significant roles in determining their performance (Anderson and Tullis, 2012; Parsaie and Haghiabi, 2014).

The flow over side weirs, spatially varied, shows a discharge decrease (De Marchi, 1934). To derive the side weir equation, the following assumptions were made, as illustrated in Fig. 1: The channel is of rectangular prismatic shape.

The side weir's brevity guarantees consistent specific energy between reaches 1 and 2. This parallels the supposition of

*Corresponding author Email: j.sadeghian@basu.ac.ir

$S_0-S_f=0$, or, $S_0=0$ and $S_f=0$. The findings from the experiment confirm this assumption (Abrishami and Hosseini, 2017).

1. The sharp-edged weir with full aeration and free surface outflow is functionally identical to a side weir.
2. The value of the energy correction factor α is 1.

Based on the stated assumptions, the governing dynamic equation for the weirs is expressed as follows Eq. 1 (Abrishami and Hosseini, 2017).

$$x = \frac{3B}{2C_m} \left[\frac{2E-3W}{E-W} \sqrt{\frac{E-y}{y-W}} - 3\sin^{-1} \sqrt{\frac{E-y}{E-W}} \right] + c \quad (1)$$

The De Marchi equation (Eq. 1) establishes a correlation between upstream and downstream depth (y), energy (E), weir height (W), channel width (B), and flow discharge coefficient (C_m). If it is required to calculate the distance between sections 1 and 2 (L), x_1 and x_2 are calculated by having Q_1 , Q_2 , y_1 and y_2 and then, the weir length is determined from their difference. In determining the length (L), removing the integral constant has no effect, and considering this, the discharge passed over the weir (Q_s) is equal to:

$$Q_s = Q_1 - Q_2 \quad (2)$$

The widespread usability of Eq. 1 enables its effective employment in calculating the discharge coefficient of nonlinear side weirs (Abrishami and Hosseini, 2017).

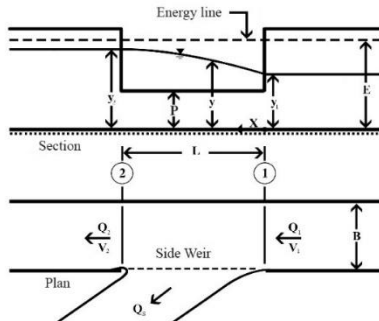


Fig. 1. A schematic illustration depicting a side weir. (Abrishami and Hosseini, 2017).

Research into the discharge coefficient of labyrinth weirs was scant before 1970, although Gentilini, Tison, and Franson made notable contributions. Subsequently, Taylor was the first to undertake a comprehensive and systematic study of labyrinth weirs discharge coefficient (Monjezi et al., 2018). Labyrinth weirs exhibit various geometric configurations; however, they are generally classified into three primary categories based on the shape of their cycles: triangular, trapezoidal, and rectangular labyrinth weirs (Fig. 2) (Falvey, 2002).

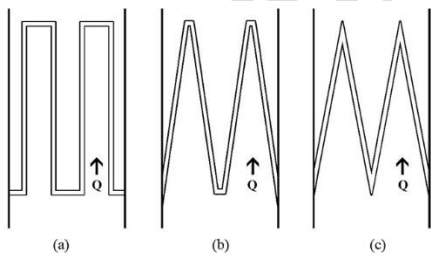


Fig. 2. General classification of the labyrinth weirs: (a) rectangular, (b) trapezoidal, and (c) triangular (Falvey, 2002).

An empirical equation for the calculation of labyrinth weir discharge coefficients was presented by Darvas (1971), which established a foundation for subsequent design curves (Darvas, 1971). Later Magalhães and Lorena (1989) developed similar curves, expanding upon Darvas's work for labyrinth weirs. Their studies culminated in the presentation of a dimensionless discharge coefficient, defined as follows (Falvey, 2002).

$$C_d = \frac{Q}{W \cdot \sqrt{2g} \cdot H_t^{3/2}} \quad (3)$$

The parameters for this analysis are defined as follows: discharge coefficient (C_d), discharge (Q), weir opening length (W), total head (H_t), and gravitational acceleration (g). Eq. 4, a dimensionless coefficient for calculating labyrinth weir discharge, was introduced by Waldron based on a prototype study conducted at Standley Lake (Tullis et al., 1995).

$$C_d = \frac{3Q}{2L_e \cdot \sqrt{2g} \cdot H_t^{3/2}} \quad (4)$$

The weir's discharge coefficient (C_d), discharge (Q), effective length (L_e), total flow height (H_t), and gravitational acceleration (g) are defined as follows. Eq. 4 was used to calculate the discharge coefficient for all nonlinear side weirs, including piano key and labyrinth side weirs.

An experimental investigation of the discharge coefficient of triangular side weirs in single-cycle and two-cycle configurations was performed by (Borghi et al., 2013), with a particular emphasis on subcritical flow conditions. The study's variables included weir opening length, notch angle, and number of cycles, weir height, and upstream flow depth. Results show a performance advantage of triangular labyrinth side weirs over linear weirs. The hydraulic performance of trapezoidal labyrinth side weirs operating in a two-cycle mode under subcritical flow regimes was analyzed by (Emiroglu et al., 2014). Their study examined the discharge coefficient in both single-cycle and multi-cycle configurations, with a focus on fixed opening and crest lengths. By analyzing their results and employing the De Marchi equation, they derived formulas to calculate the discharge coefficient for trapezoidal labyrinth side weirs. Moreover, a unique equation is needed for calculating the discharge coefficient for each labyrinth side weir configuration. Lempérière and Ouamane (2003) developed an improved labyrinth weir, the design of which resembled piano keys, leading to its nomenclature as the piano key weir (PKW). France's Goulours Dam, under EDF (French Ministry of Water and Electricity), saw the first implementation of this innovative design in 2006. As a novel subclass of labyrinth weirs, PKWs have been shown through studies to exhibit a high capacity for passing significant flow volumes. Studies conducted by the Hydrocoop Institute and the University of Biskra on various PKW designs highlighted several advantages, as reported by (Lempérière and Ouamane, 2003; Anderson, 2011). Weirs hydraulic performance is intricate because of differing shapes, types, and the multiple parameters impacting the structure's discharge coefficient. Therefore, developing physical models of the weirs is a step forward (Anderson, 2011). The PKWs are classified into 4 groups based on the console advancement, rather than the presence or absence of the weir overhangs. Fig. 3 shows that A-type PKWs have both downstream and upstream overhangs, while type B and C PKWs lack either or both, respectively. Type D PKW refers to weirs lacking both upstream and downstream overhangs.

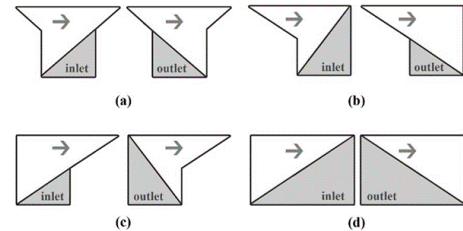


Fig. 3. (a) A-Type, (b) B-Type, (c) C-Type, and (d) D-Type PKWs (Lempérière and Ouamane, 2003).

A three-dimensional representation of the PKW, including its primary parameters, is shown in Fig. 4. In Fig. 4, W denotes the total width of the weir, W_o refers to the width of the outlet key, and W_i shows the width of the inlet key. T_s stands for the thickness of the weir, while W_u represents the width of a single cycle. P_i is the height of the weir's inlet key, and P_o corresponds to the height of the outlet key. B signifies the overall length of the weir, B_b is the foundation length, and B_o and B_i represent the lengths of the downstream and upstream overhangs, respectively.

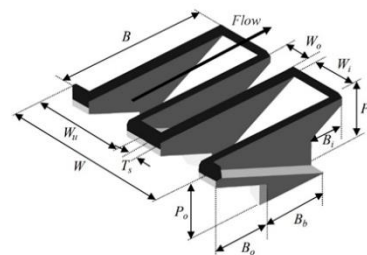


Fig. 4. The PKW's main parameters are shown in a 3D-view (Pralong et al., 2011).

Machiels (2012) conducted extensive studies on the PKWs using the experimental models with 1.5, 2.5 and 3.5 cycles. The experiments were conducted in a channel with dimensions of 7.2 m, 1.2 m in width,

and 1.2 m in height and found that at low H/P ratios, the flow jet transformation, such as the transformation of the sticky jet into the compact jet, and from the compact jet into the free jet, was observed on the PKW. Transformations depend on the shape and thickness of the PKW crest.

They also studied the effect of shield walls on the PKW efficiency, and the results showed that the weir efficiency for the developed models with $P/W_u = 0.34$ was higher than that of the models with $P/W_u = 1.33$, and also suggested the optimal value of P/W as 1.33 (Machiels, 2012). According to Mehboudi et al. (2016), an analysis of the effective geometric parameters on the discharge coefficient of trapezoidal PKWs, considering different flow conditions, identified L/W and W_i/W_o parameters as the most and least effective parameters (Mehboudi et al., 2016). Seyed Javad et al. (2019) conducted a study on 16 trapezoidal side PKW models with heights of 10, 15, and 20 cm in a channel with specific dimensions. The study found that trapezoidal side PKWs outperformed rectangular side PKWs and linear weirs in terms of discharge coefficient. They also observed that increasing the width of the weir resulted in higher discharge capacities (Seyed Javad et al., 2019). Karimi et al. (2017) examined the discharge coefficient for nine C-Type side PKWs, employing a 10 m long, 60 cm high, and 60 cm wide channel made of 4 mm thick glass, and analyzing various geometries. The study assessed the discharge coefficient of side PKWs with rectangular side weirs, revealing that side PKWs exhibited notably superior discharge capacities. The study showed that the discharge coefficient exhibited a decline in response to elevated upstream Froude numbers, flow heights, and H/P ratios surpassing 0.5. In addition, a higher L/W ratio caused increased discharge capacities in the side PKWs (Karimi et al., 2017). Saghari et al. (2019) researched the discharge coefficient of A-type trapezoidal side PKWs in curved rectangular channels under subcritical flow; they discovered that the TPKSWs coefficient was about 2.68 times larger than that of LRSWs (Saghari et al., 2019). Mehri et al. (2020) investigated how rectangular side PKWs (types A, B, C, and D) performed within a 120° segment of a 180° curved channel. Type B weir outperformed A, C, and D weirs, with discharge coefficients 9.9%, 21.2%, and 24.1% higher, respectively (Mehri et al., 2020). Kilic and Emiroglu (2022) compared three approaches (De Marchi, Schmidt, Dominguez) to analyze trapezoidal side PKW hydraulics, concluding that trapezoidal labyrinth side weirs have higher discharge coefficients than trapezoidal side PKWs when $0.38 < Fr < 0.76$ (Kilic and Emiroglu, 2022). Previous research highlights the significance of studying discharge coefficients for both labyrinth and piano key side weirs, despite limited research in this area. This study examines the discharge coefficient for A-type piano key weirs and trapezoidal, triangular, and rectangular labyrinth weirs. The following sections outline the models, laboratory apparatus, testing methodologies, and comparisons to another research. This study's novel contribution is a comprehensive experimental comparison of A-type piano key weirs against three labyrinth side weir configurations (with varying heights) under side-channel flow, a topic not widely researched.

2. Materials and methodologies

This section first identifies parameters influencing the tests using dimensional analysis, then describes the lab equipment and models.

2.1. Dimensional analysis

The discharge coefficient for labyrinth and piano key weirs is a function of the following factors, besides gravity (g) and the De Marchi coefficient (C_m).

A) Density (ρ), dynamic viscosity (μ), density (ρ), and surface tension (σ) are the fluid's key physical properties.

B) The hydraulic properties, including upstream and downstream flow depths (y_1, y_2) and velocities (v_1, v_2) (calculated from discharge and channel geometry), can function as either dependent or independent variables.

C) The channel and weir geometry's parameters include weir opening length (W), effective length (L_e), weir height (P), inlet and outlet key widths (W_i and W_o), installation angle (α), side slope angle (δ), upstream and downstream overhang lengths (B_i and B_o), width (B), main channel bed slope (S_0), and the number and shape of cycles (n).

Based on the variables, we can conclude:

$$\phi_1 = (S_0, P, B_o, W, g, W_i, B, W_o, L_e, B_i, y_1, \mu, v_1, v_2, n, g, y_2, \alpha, \delta, \rho, C_m, \sigma) = 0 \quad (5)$$

Buckingham's theory suggests 16 variables; however, using upstream flow depth (L), velocity (LT^{-1}), and water density (ML^{-3}) as primary variables leaves 13 dimensionless ones. A dimensionless variable is got by combining each of the variables with the main variables.

$$C_m = \phi_1 \left(\frac{V_1^2}{gy_1}, \frac{\mu}{\rho y_1 V_1}, \frac{\sigma}{\rho y_1 V_1^2}, \frac{y_2}{y_1}, \frac{W}{y_1}, \frac{B}{y_1}, \frac{B_i}{y_1}, \frac{B_o}{y_1}, \frac{L_e}{P}, \frac{W_i}{W_o}, S_0, \delta, \alpha \right) \quad (6)$$

In the hydraulics of open channels, turbulent flow conditions render the effect of viscous forces against inertia negligible. As the flow in such channels is predominantly turbulent, the influence of viscous forces, represented by the Reynolds number ($\mu/\rho y_1 v_1$), was disregarded in this study (Seyed Javad et al., 2019). Similarly, surface tension effects are only significant for flow depths less than 3 cm. Since the flow depths in the present experiments exceeded 3 cm, the influence of surface tension, represented by the Weber number ($\sigma/\rho y_1 v_1^2$), was also neglected (Kazemi et al., 2016). Additionally, some researchers have noted that the channel bed slope has an insignificant effect under subcritical flow conditions (Razmi et al., 2022). This study excluded the channel bed slope's effect because all upstream Froude numbers were below one, signifying subcritical flow. Considering the influence of dimensionless variables and their integration with other parameters, Eq. 7 was derived.

$$C_m = \phi_2 \left(Fr_2, \frac{y_2}{y_1}, \frac{W}{B}, \frac{P}{y_1}, \frac{L}{W}, \frac{B_i}{W}, \frac{B_o}{W}, \frac{L_e}{P}, \frac{W_i}{y_1}, S_0, \delta, \alpha \right) \quad (7)$$

2.2. Experimental setup

Experimental labyrinth side weir models, encompassing rectangular, triangular, trapezoidal, and Type A piano key configurations, were constructed with three cycles and four heights of 5, 10, 15, and 20 cm. These models were built with a 57 cm opening length and constructed from plexiglass sheets of 5 mm thickness.

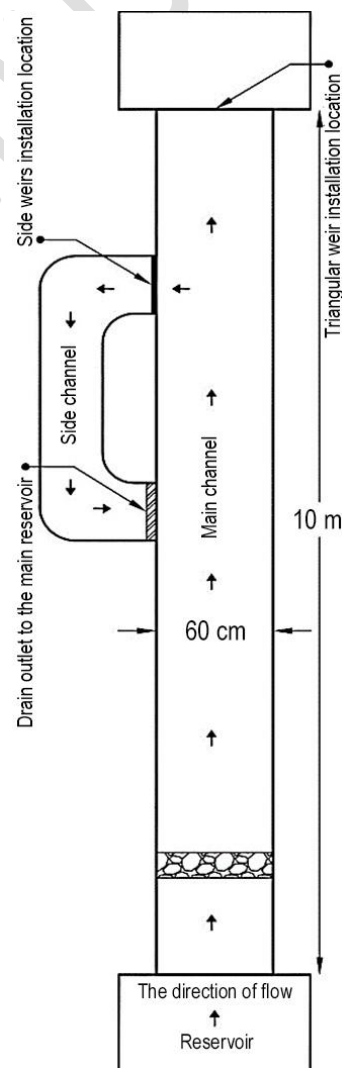


Fig. 5. Plan of the 10 m experimental channel.

Using a 10 m long, 60 cm wide, and 60 cm high channel in Bu-Ali Sina University's hydraulics lab, the experiments were performed. Glass sidewalls and a glass floor gave a clear view of the flow within the channel. Water was pumped from a reservoir into the channel, and upon overflowing from the weirs, it was returned to the main tank either directly or via a side channel. To minimize turbulence in the inflow to

the main channel, a grid composed of mesh bricks reinforced with metal nets was installed upstream of the channel. To determine flow discharge, a calibrated triangular weir was employed, positioned downstream of the main channel. The experimental setup included precise measuring equipment to ensure accurate data collection. Water depth measurements at the side weirs used a point gauge accurate to within ± 0.1 mm. A calibrated triangular weir measured the discharge, accurate to within $\pm 1.5\%$. In addition, a pump regulated the main channel's flow rate, which was measured using calibrated stage-discharge curves from rectangular and triangular weirs at the channel's outlet. All equipment was calibrated prior to the experiments to minimize errors and ensure the reliability of the results. Fig. 5 shows the experimental setup of the main and side channels. A point depth gauge (accuracy 0.1 mm) measured flow depth upstream of the weirs (Fig. 6). Eq. 4 was employed in order to determine the discharge coefficient of the side weirs. Table 1 shows the characteristics of the weir and the performed experiments. The main and side channels are visually depicted in Fig. 7, with Figs. 8–11 displaying example weirs.



Fig. 6. Depth gauge.



Fig. 7. 10 m channel and side channel view.



(a)



(b)

Fig. 8. Water flow over the triangular labyrinth side weir; where (a) $P = 5$ cm and (b) $P = 10$ cm.



(a)



(b)

Fig. 9. Water flow over the trapezoidal labyrinth side weir; where (a) $P = 5$ cm and (b) $P = 15$ cm.



(a)



(b)

Fig. 10. Water flow over the rectangular labyrinth side weir; where (a) $P = 15$ cm and (b) $P = 20$ cm.



(a)



(b)

Fig. 11. Water flow over the piano key side weir; where (a) $P = 15$ cm and (b) $P = 20$ cm.

Table 1. Side weir models: characteristics and testing.

Weir type	W, cm	P, cm	L_s/W	L, cm	Q_L , l/s	C_d	Fr_1
Piano Key SW	57	5,10,15,20	3.47	198	2.41 - 23.59	0.123 - 0.373	0.016 - 0.242
Rectangular LSW	57	5,10,15,20	3.47	198	1.33 - 20.47	0.135 - 0.535	0.011 - 0.263
Triangular LSW	57	5,10,15,20	1.41	80.6	2.49 - 9.40	0.185 - 0.689	0.014 - 0.190
Trapezoidal LSW	57	5,10,15,20	2.20	125.5	2.57 - 15.50	0.086 - 0.664	0.015 - 0.229

3. Results and discussion

This section presents the results of experimental tests conducted on diverse labyrinth and piano key side weirs. The analysis focuses on the relationship between the discharge coefficient and H/P ratio, followed by an evaluation of the efficiency R of each weir configuration.

3.1. Labyrinth and the piano key side weirs

Fig. 12 presents the C_d changes relative to H/P for the 16 models of trapezoidal, rectangular, and triangular rectangular LSWs and PKWs with 5, 10, 15, and 20 cm heights. As it can be seen, changes of C_d are inversely related to H/P , and in each weir, C_d take the maximum value for smaller values of H/P . By increasing H/P , because of interference of flow nappes at high levels, C_d decrease. This decreasing trend was milder for shorter weirs and sharper for taller weirs. Within the triangular labyrinth side weirs, the 5 cm height variant presented the highest discharge coefficient when assessing coefficient variations in relation to H/P alterations. Specifically, the discharge coefficient exceeded those of the weirs with heights of 10, 15, and 20 cm by 17.9%, 22.3%, and 26.8%, respectively. For triangular labyrinth weirs with heights of 5, 10, 15, and 20 cm, respectively, an increase in the H/P ratio beyond the values of 0.69, 0.27, 0.17, and 0.12, results in a deviation from the

weir's optimal performance. Within the trapezoidal labyrinth weirs, the discharge coefficient of the weir with a 5 cm height increased by 11.5%, 14.4%, and 17.9%, compared to the coefficients of the 10, 15, and 20 cm weirs. The higher discharge coefficient and efficiency of the weir with a height of 5 cm, compared to other similar weirs, can be attributed to the less steep decline in C_d as H/P increases. In the trapezoidal labyrinth weirs, the optimal performance saw a marked decrease in efficiency when H/P values exceeded 0.82, 0.41, 0.29, and 0.19 for the corresponding heights of 5, 10, 15, and 20 cm. The discharge coefficient for the rectangular labyrinth weir with a height of 20 cm was 34%, 7.3% and 14.1% higher than that of the same type weirs with a height of 5, 10 and 15 cm respectively. In rectangular labyrinth weirs with heights of 5, 10, 15, and 20 cm, the weir efficiency significantly decreased from its optimal performance and behaved linearly for H/P values exceeding 0.95, 0.66, 0.46, and 0.32, respectively. In the PKWs, the discharge coefficient of the weir with a height of 15 cm was enhanced by 9.3%, 5.5%, and 9.2% when compared to the same type of weir with a height of 5, 10, and 20 cm, correspondingly. For PKWs with heights of 5, 10, 15, and 20 cm, a significant decrease in weir efficiency from optimal performance was observed, and the weir performed linearly, when H/P values exceeded 0.88, 0.6, 0.44, and 0.35, respectively.

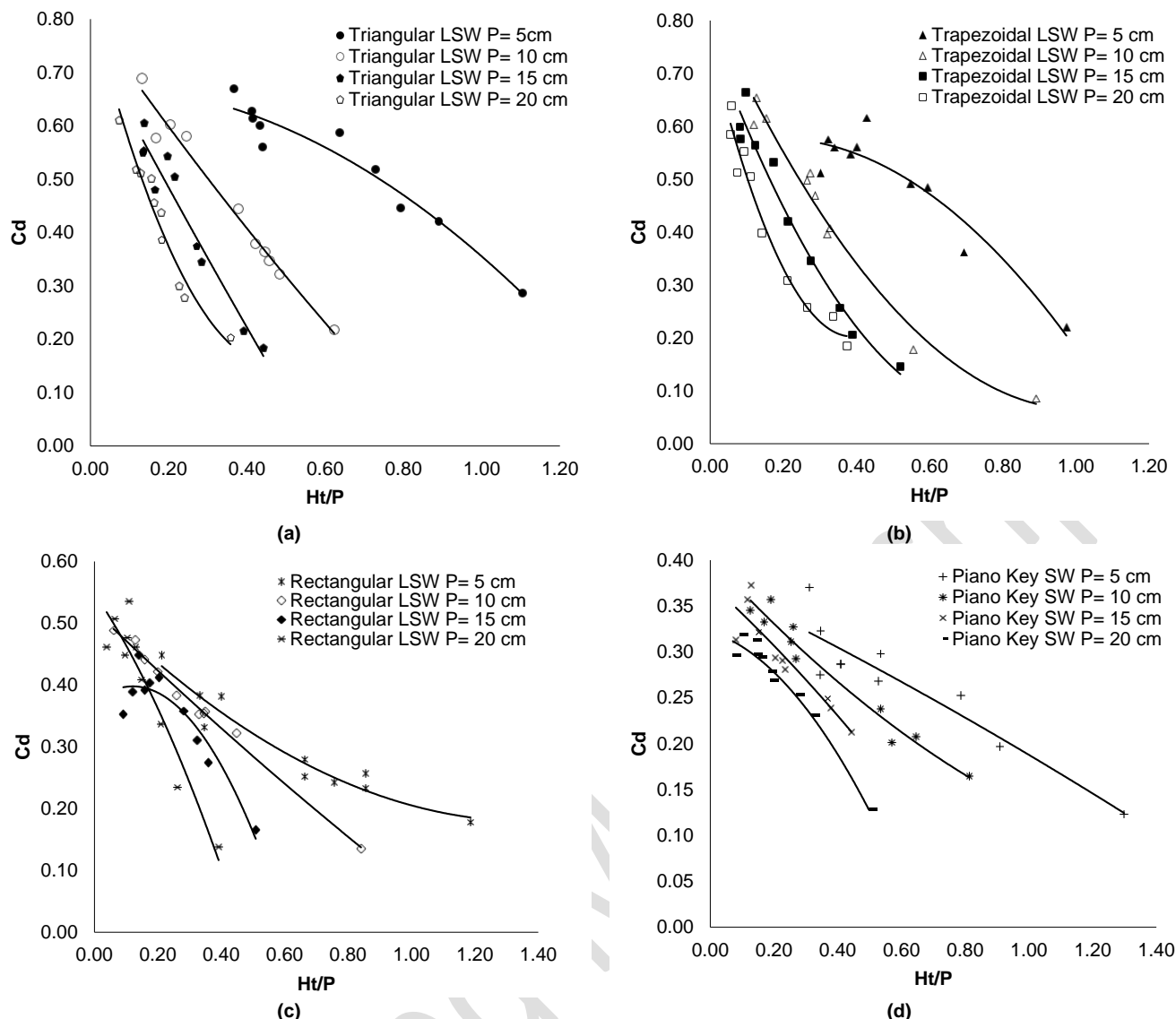


Fig. 12. Changes of C_d versus H_t/P in side weirs; (a) Triangular LSW, (b) Trapezoidal LSW, (c) Rectangular LSW, and (d) Piano Key SW.

Weirs exhibiting the highest average discharge coefficient relative to other weirs of the same model were selected to compare the discharge coefficient C_d with the H_t/P ratio across all weirs. According to the data presented in Fig. 13, the triangular labyrinth side weir's discharge coefficient was enhanced by 7.56%, 24.85%, and 45.05% compared to the trapezoidal, rectangular, and piano key labyrinth side weirs, correspondingly.

3.2. Efficiency of the side weirs

Hay and Taylor (1970) determined that the weir's discharge performance, represented as Q_L/Q_n , is solely reliant on the parameters H_t/P , W/P , L/W , α , and n (Hay and Taylor, 1970). To compare the efficiency of the side weirs for changes in H_t/P ratio, parameter R was defined and used.

$$R = \left[(Q_L / Q_n) / (L / W) \right] * 100 \quad (8)$$

The variables are defined as follows: R is the weir efficiency; Q_L is the discharge over the labyrinth or piano key side weir; Q_n is the discharge over the linear side weir; L is the effective weir length (total weir crest length); and W is the weir's opening length. Fig. 14 presents the relationship between R and H_t/P for trapezoidal, triangular, rectangular labyrinth side weirs, and piano key side weirs, with heights of 5, 10, 15, and 20 cm. In weirs with a height of 5 cm, the triangular labyrinth weir is more efficient than other weirs of the same height and has the highest efficiency in a fixed H_t/P ratio. The piano key side weir has the lowest efficiency at this height compared to other weirs. Among the weirs with a height of 5 cm, the efficiency of the triangular labyrinth weir decreased earlier than other weirs of the same height, and this happened for the rectangular labyrinth weir later than other weirs. In weirs with a height of 10 cm, the decreasing trend of changes of R versus H_t/P in the triangular and trapezoidal weirs increased compared

to that of the rectangular labyrinth side weirs and piano key side weirs, and the efficiency decreased with more intensity.

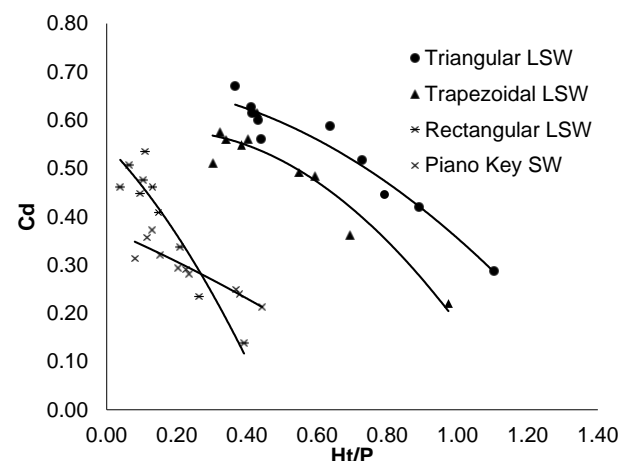


Fig. 13. Changes of C_d vs. H_t/P for weirs with the best performance compared to similar type weirs

The triangular labyrinth weir is more efficient than the trapezoidal labyrinth weir. In addition, for H_t/P values less than 0.58 and 0.63, this type of weir had a higher efficiency than the rectangular labyrinth side weirs and the piano key side weirs, respectively. For H_t/P values less than 0.42 and 0.54, the trapezoidal labyrinth weir had a higher efficiency than the rectangular labyrinth and the piano key weirs, and its efficiency decreased with the H_t/P ratio. The rectangular labyrinth weir exhibited greater efficiency compared to the piano key weir for $H_t/P < 0.74$. In weirs with a height of 15 cm, the efficiency changes versus H_t/P for all 4 types

of weirs was descending; however, these changes were more intense in the trapezoidal and triangular labyrinth weirs compared to the other two types of weirs. For H_t/P values less than 0.40, 0.31 and 0.39, the triangular labyrinth weir had higher efficiency than the trapezoidal labyrinth, rectangular labyrinth and piano key weirs, respectively. The trapezoidal labyrinth weir also had the same efficiency as the rectangular labyrinth and the piano key weirs in H_t/P values of 0.26 and 0.38, and by increasing and decreasing H_t/P values, its efficiency decreased compared to the rectangular labyrinth weir but increased compared to the piano key weir. The rectangular labyrinth and the piano key side weirs also had the same efficiency at $H_t/P=0.47$, and at $H_t/P<0.47$, the rectangular labyrinth weir had better efficiency. In weirs with a height of 20 cm, the efficiency decreased with increasing H_t/P for all four weir types of weirs was descending with more intense changes than other weir heights. The triangular labyrinth weir in H_t/P values less than 0.32, 0.31 and 0.30 had higher efficiency than the trapezoidal labyrinth, rectangular labyrinth and the piano key side weir, respectively and by increasing the H_t/P values, it had lower efficiency than other weirs. The trapezoidal labyrinth side weir had the same efficiency as the rectangular labyrinth and piano key side weirs in H_t/P values of 0.32 and 0.27, and by increasing and decreasing these values, it had a lower and higher efficiency than the mentioned weirs, respectively. In

addition, the rate of efficiency reduction with increasing H_t/P was greater in the trapezoidal labyrinth weir than in other weir types. By comparing the rectangular labyrinth and the piano key side weirs, the changes of efficiency versus H_t/P were more intense in the rectangular labyrinth weir and in $H_t/P=0.30$, the weirs had equal efficiency and by increasing H_t/P , the rectangular labyrinth weir had lower efficiency than the PKW. The geometric design of the triangular labyrinth weir contributes to its superior performance. Its shape optimizes flow efficiency by minimizing flow separation and turbulence at the crest. In addition, its geometry maximizes the effective crest length relative to channel width (L/W), enabling greater discharge capacity compared to other weir types. This configuration also reduces interference between flow nappes, particularly at lower H_t/P ratios, resulting in smoother and more efficient flow over the crest. Furthermore, the geometric arrangement of the triangular labyrinth weir ensures consistent performance over a wide range of H_t/P values, with the most significant gains observed at moderate H_t/P ratios (e.g., 0.4–0.6). These design characteristics explain the superior performance of triangular labyrinth weirs under the tested conditions, supporting their application in scenarios requiring high discharge efficiency. This conclusion aligns with findings in existing literature, which also highlight the efficiency advantages of triangular configurations in labyrinth weirs.

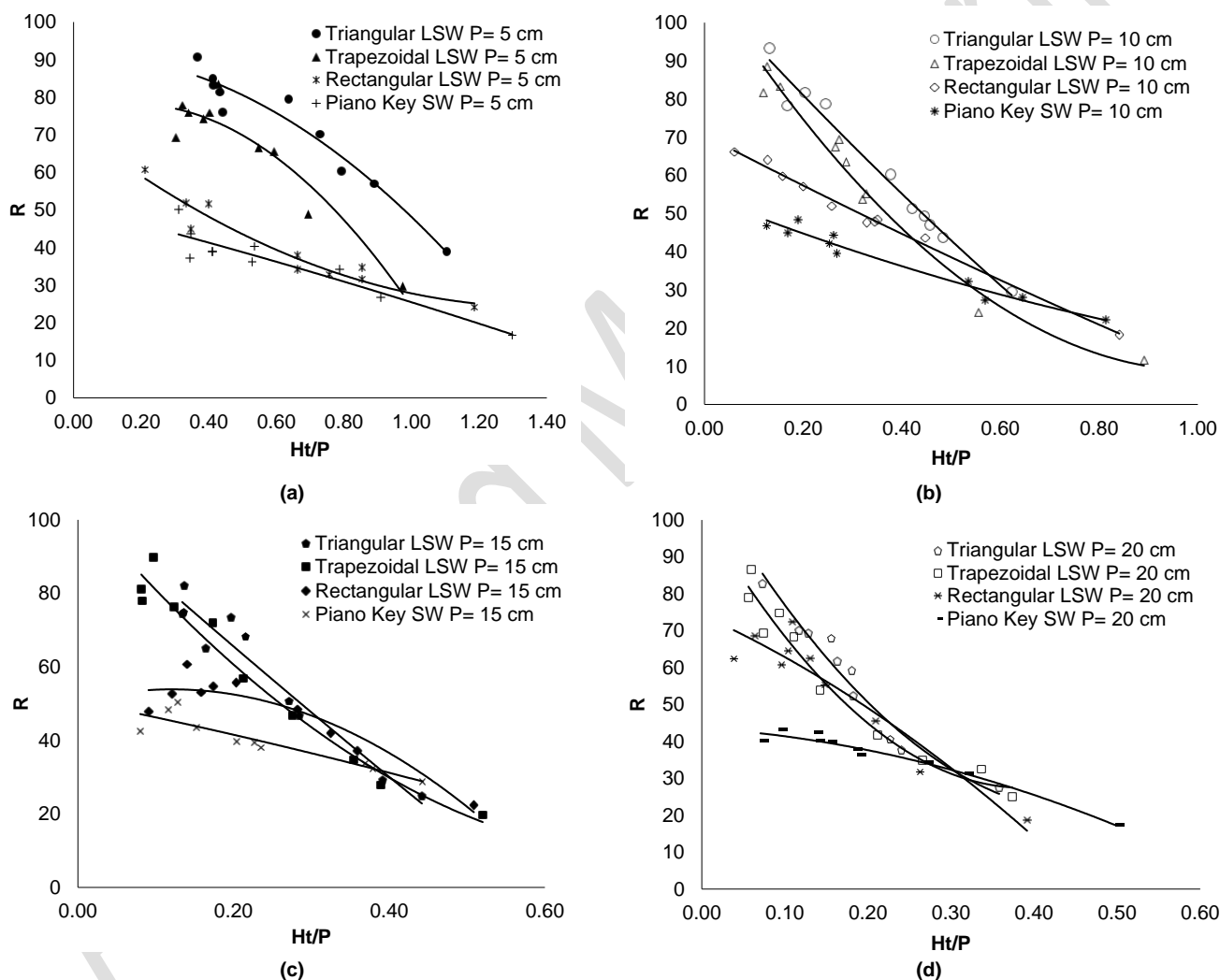


Fig. 14. Changes of R versus H_t/P in side weirs; (a) $P=5$ cm, (b) $P=10$ cm, (c) $P=15$ cm, and (d) $P=20$ cm.

In order to compare the changes of efficiency, R versus H_t/P in all weir types, the weirs with the maximum efficiency on average compared to other weirs of the same model were selected. According to Fig. 15, the efficiency of the triangular labyrinth side weir increased by 7.56%, 24.85%, and 45.05% compared to that of the trapezoidal, rectangular, and piano key labyrinth side weirs, respectively. These percentages represent the relative increases in efficiency based on the average performance observed across the tested H_t/P range. The data presented in Fig. 15 confirms these trends, highlighting the superior performance of triangular labyrinth weirs under the tested condition. Based on the performed comparisons, the triangular labyrinth side weir had the highest value of R compared to other side weirs. Fig. 15 Comparison of the efficiency of triangular, trapezoidal, rectangular, and

piano key labyrinth side weirs. The percentages (7.56%, 24.85%, and 45.05%) represent the average increases in efficiency of the triangular labyrinth side weir relative to trapezoidal, rectangular, and piano key side weirs, respectively, across the entire tested H_t/P range (0.2 to 0.8). These trends are most pronounced at moderate H_t/P values (0.4–0.6), where the advantages of the triangular geometry are maximized. The analysis revealed that specific weir shapes outperform others under certain conditions.

Triangular labyrinth weirs consistently showed the highest efficiency at lower H_t/P ratios, where their discharge coefficient was up to 26.8% higher compared to trapezoidal, rectangular, and piano key side weirs. This efficiency is attributed to their streamlined geometry, which minimizes flow interference and enhances discharge at lower

flow depths. Rectangular labyrinth weirs exhibited superior performance in side-channel configurations, particularly at moderate to high H_t/P ratios (e.g., $H_t/P = 0.3$).

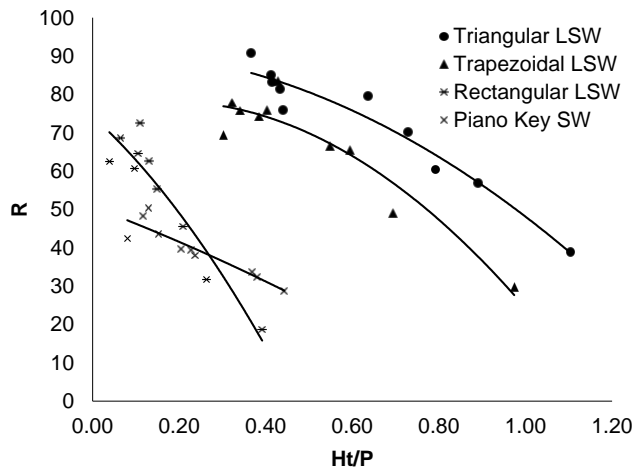


Fig. 15. Changes of R vs. H_t/P for weirs with the best performance compared to similar type weirs.

Their performance was approximately 15% better than piano key side weirs under these conditions, likely because of their larger effective crest length, which accommodates higher discharge rates without significant flow interference. Piano key weirs, while typically more efficient in direct-channel setups as reported in previous studies, were less effective in side-channel applications. This reduced efficiency is attributed to the interference of flow nappes at higher H_t/P ratios, which diminishes their overall discharge coefficient. In conclusion, triangular labyrinth weirs are most efficient at lower H_t/P ratios, rectangular labyrinth weirs excel at moderate H_t/P ratios in side-channel configurations, and piano key weirs are more effective in direct-channel setups. The choice of weir shape should therefore be guided by the specific hydraulic and geometric conditions of the application.

4. Conclusions

Weirs are among the most critical hydraulic structures, and evaluating their discharge coefficient and efficiency is essential, particularly in locations with limited spatial constraints. The selection of weirs with higher discharge coefficients and efficiencies is crucial to ensure optimal performance. Given the significant role of lateral weirs, their discharge behavior causes the use of weirs with superior discharge coefficients. While piano key and labyrinth weirs have been extensively studied and compared as direct weirs in canals and dams, further investigation is required to evaluate their performance when used as side weirs in such systems. This research focuses on assessing the performance of these weirs as side weirs in a canal. This study's results show that trapezoidal, triangular, and rectangular labyrinth side weirs are more efficient than piano key A-type weirs when installed laterally. This contrasts with previous studies, where piano key weirs exhibited superior performance when aligned perpendicular to the flow axis. The key results of this research are summarized as follows:

1. In a certain ratio of H_t and H_t/P , weirs with a smaller height ($P = 5$ cm) had the maximum discharge coefficient, and vice versa. The triangular and trapezoidal side weirs with a smaller height had almost the same performance as the weirs perpendicular to the flow direction.
2. The At low H_t/P ratios, the falling flow nappes in labyrinth weirs remained cohesive and required aeration. As H_t/P increased, interference between the falling flow nappes gradually intensified, leading to a reduction in the discharge coefficient of the weir. For piano key side weirs and rectangular labyrinth side weirs, the interaction led to the formation of an afflux at the downstream end of the output keys; this signaled the commencement of a marked reduction in the weir's effectiveness. With further interference, the weir progressively deviated from its optimal performance and exhibited behavior similar to that of a linear weir.
3. For all weirs of the same type, such as triangular labyrinth weirs, at specific H_t/P ratios, weirs with smaller heights exhibited higher discharge coefficient and efficiency compared to those with greater heights.
4. At specific H_t/P ratios, triangular labyrinth weirs showed higher efficiency compared to other weirs of the same height. Conversely, at the same H_t/P ratios, piano key side weirs exhibited lower efficiency than the other weir types. The rate of change in discharge coefficient and efficiency for triangular labyrinth side

weirs was more pronounced compared to trapezoidal and rectangular labyrinth side weirs, as well as piano key side weirs. As the H_t/P ratio increased, the discharge coefficient and efficiency of triangular labyrinth side weirs declined at a faster rate than the other weir types.

5. Piano key straight weirs showed higher efficiency compared to rectangular labyrinth weirs. However, the opposite trend was observed for side weirs, where, on average, rectangular labyrinth side weirs exhibited superior efficiency compared to piano key side weir.
6. Under conditions of side-flow, triangular labyrinth side weirs exhibited up to 45.05% greater efficiency than piano key weirs, and rectangular labyrinth weirs outperformed piano key weirs by roughly 24.85%.

Nomenclature

B	Width of the main channel
B_i	Upstream overhang length
B_o	Downstream overhang length
C_d	Discharge coefficient
C_m	De Marchi coefficient
Fr_1	Froude number
g	Acceleration of gravity (gravity acceleration)
H_t	Flow depth over the weir
L	total length of the weir crest
L_e	Weir effective length (total length of the weir crest)
P	Weir height
Q_L	Discharge passing over the side weir
Q_n	Discharge passing over the linear weir
Q_s	Side weir discharge
R	Weir operational efficiency
S_o	The slope of the channel's bottom
S_f	The energy line's slope
V_1	The velocity at the upstream section of the side weir
V_2	The velocity at the downstream section of the side weir
W	Weir opening length
W_i	Inlet key's width
W_o	Outlet t key's width
y_1	Height in the upstream cross section of the side weir
y_2	Height in the downstream cross section of the side weir
y_c	Critical height
y_t	Tailwater depth
α	Energy correction factor

Author Contributions

Saeid Jeddi: Contributed to the study conception and design, conducted material preparation, data collection, and analysis, and composed the first draft of the manuscript.

Jalal Sadeghian: Contributed to the study conception and design, conducted material preparation, data collection, and analysis, and provided feedback on prior versions of the manuscript.

Conflict of Interest

The authors have no competing interests to declare, including non-financial ones.

Acknowledgement

The author is grateful for the data support provided by the hydraulic laboratory at Bu-Ali Sina University.

Data Availability Statement

Datasets employed and/or evaluated in this research are available from the corresponding author upon justifiable request.

References

- Abreshami, J. and Hosseini, M. (2017) *Hydraulic open canals*. 19th edn. Mashhad: Mashhad University Press (In Persian).
- Anderson, R.M. (2011) *Piano key weir head discharge relationships*. MS Thesis, Utah State University. Available at: <https://doi.org/10.26076/ce75-6c42> (Accessed date: 11 April 2025).
- Anderson, R.M. and Tullis, B.P. (2012) 'Comparison of piano key and rectangular labyrinth weir hydraulics', *Journal of Irrigation and Drainage Engineering*, 138(4), pp. 358–361. doi: [https://doi.org/10.1061/\(ASCE\)HY.1943-7900.0000509](https://doi.org/10.1061/(ASCE)HY.1943-7900.0000509)

- Borghei, S.M. et al. (2013) 'Triangular labyrinth side weirs with one, and two cycles', *Proceedings of the Institution of Civil Engineers - Water Management*, 166(1), pp. 27–42. doi: <https://doi.org/10.1680/wama.11.00032>
- Darvas, L.A. (1971) 'Discussion of Performance and design of labyrinth weirs by Hay and Taylor', *Journal of Hydraulic Engineering*, 97(8), pp. 1246–1251. doi: <https://doi.org/10.1061/JYCEAJ.0003056>
- De Marchi, G. (1934) 'Saggio di teoria del funzionamento degli stramazzi laterali (theoretical knowledge on the functioning of side weirs)', *L'energia Elettrica*, 11(11), pp. 849-860 (in Italian). Available at: <https://cir.nii.ac.jp/crid/1573950399565609344> (Accessed date: 15 June 2025).
- Emiroglu, M.E. et al. (2014) 'Discharge characteristics of a trapezoidal labyrinth side weir with one and two cycles in subcritical flow', *Journal of Irrigation and Drainage Engineering*, 140(5), pp. 243–254. doi: [https://doi.org/10.1061/\(ASCE\)IR.1943-4774.000070](https://doi.org/10.1061/(ASCE)IR.1943-4774.000070)
- Falvey, H.T., (2002) *Hydraulic design of labyrinth weirs*. Reston, VA: ASCE Press.
- Hay, N. and Taylor, G. (1970) 'Performance and design of labyrinth weirs', *Journal of the Hydraulics Division*, 96(11), pp. 2337–2357. doi: <https://doi.org/10.1061/JYCEAJ.0002766>
- Karimi, M. et al. (2017) 'Experimental study of discharge coefficient of a Piano Key Side Weir', *Labyrinth and Piano Key Weirs III: Proceedings of the 3rd International Workshop on Labyrinth and Piano Key Weirs (PKW 2017)*, Qui Nhon, Vietnam. 22-24 February 2017, London: CRC Press. pp. 109–116. doi: <https://doi.org/10.1201/9781315169064>
- Kazemi, J. et al. (2016) 'The effect of the scale on the profile of the water surface in an Ogee Weir with curvature in plan and with converging lateral walls', *Journal of Applied Research of Irrigation and Drainage Structures Engineering*, 17(66), pp. 119–136. doi: <https://doi.org/10.22092/aridse.2016.106417>
- Kilic, Z. and Emiroglu, M.E. (2022) 'Study of hydraulic characteristics of trapezoidal piano key side weir using different approaches', *Water Supply*, 22(8), pp. 6672–6691. doi: <https://doi.org/10.2166/ws.2022.264>
- Lempérière, F. and Ouamane, A., (2003) 'The Piano Keys weir: a new cost-effective solution for spillways'. *International Journal on Hydropower & Dams*, 10(5), pp. 144-149. Available at: <http://www.hydrocoop.org/piano-keys-weir-a-new-cost-effective-solution-for-spillways/> (Accessed date: 18 July 2025).
- Machiels, O. (2012) *Experimental study of the hydraulic behavior of Piano key weir*, PhD Thesis. University of Liège. Available at: <https://orbi.uliege.be/handle/2268/128006> (Accessed date: 27 June 2025)
- Mehboudi, A. et al. (2016) 'Experimental study of discharge coefficient for trapezoidal piano key weirs', *Flow Measurement and Instrumentation*, 50, pp. 65–72. doi: <https://doi.org/10.1016/j.flowmeasinst.2016.06.005>
- Mehri, Y. et al. (2020) 'Experimental study and performance comparison on various types of rectangular piano key side weirs at a 120° section of a 180° curved channel', *Applied Water Science*, 10, p. 222. doi: <https://doi.org/10.1007/s13201-020-01306-z>
- Monjezi, R. et al. (2018) 'Laboratory investigation of the discharge coefficient of flow in arced labyrinth weirs with triangular plans', *Flow Measurement and Instrumentation*, 64, pp. 64–70. doi: <https://doi.org/10.1016/j.flowmeasinst.2018.10.011>
- Parsaie, A. and Haghiabi, A.H. (2014) 'Assessment of some famous empirical equation and artificial intelligent model (MLP, ANFIS) to predicting the side weir discharge coefficient', *Journal of Applied Research in Water and Wastewater*, 1(2), pp. 74-79. Available at: https://arww.razi.ac.ir/article_56.html (Accessed date: 10 May 2025).
- Pralong, J. et al. (2011) 'A naming convention for the piano key weirs geometrical parameters', *Labyrinth and piano key weirs - PKW 2011: proceedings of the international conference on labyrinth and piano key weirs (PKW 2011)*, Liège, Belgium, 9-11 February, Netherlands: CRC Press. pp. 271–278. Available at: <https://orbi.uliege.be/handle/2268/91433> (Accessed date: 19 May 2025).
- Razmi, M. et al. (2022) 'Comparative evaluation of CFD model and intelligence hybrid method to ameliorate ANFIS in side weir coefficient of discharge modelling', *Journal of Applied Research in Water and Wastewater*, 9(2), pp. 125-140. doi: <https://doi.org/10.22126/arww.2023.7934.1255>
- Saghari, A. et al. (2019) 'Experimental study of trapezoidal piano key side weirs in a curved channel', *Flow Measurement and Instrumentation*, 70, p. 101640. doi: <https://doi.org/10.1016/j.flowmeasinst.2019.101640>
- Seyed Javad, M. et al. (2019) 'Experimental study of discharge coefficient of a trapezoidal piano key side weir', *Journal of Hydraulics*, 14(2), pp. 33–46. doi: [10.30482/jhyd.2019.152034.1332](https://doi.org/10.30482/jhyd.2019.152034.1332)
- Tullis, J.P. et al. (1995) 'Design of labyrinth spillways', *Journal of Hydraulic Engineering*, ASCE, 121(3), pp. 247–255. doi: [https://doi.org/10.1061/\(ASCE\)0733-9429\(1995\)121:3\(247\)](https://doi.org/10.1061/(ASCE)0733-9429(1995)121:3(247))